Clim Dyn (2018) 51:4065–4076
DOI 10.1007/s00382-017-3669-y

Enhanced influence of early-spring tropical Indian Ocean SST on the following early-summer precipitation over Northeast China

Tingting Han[1,2,4] · **Shengping He**[1,2,3,5] · **Huijun Wang**[1,2,3] · **Xin Hao**[1,2,4]

Received: 30 December 2016 / Accepted: 30 March 2017 / Published online: 8 April 2017

Abstract The relationship between the tropical Indian Ocean (TIO) and East Asian summer monsoon/precipitation has been documented in many studies. However, the precursor signals of summer precipitation in the TIO sea surface temperature (SST), which is important for climate prediction, have drawn little attention. This study identified a strong relationship between early-spring TIO SST and subsequent early-summer precipitation in Northeast China (NEC) since the late 1980s. For 1961–1986, the correlations between early-spring TIO SST and early-summer NEC precipitation were statistically insignificant; for 1989–2014, they were positively significant. Since the late 1980s, the early-spring positive TIO SST anomaly was generally followed by a significant anomalous anticyclone over Japan; that facilitated anomalous southerly winds over NEC, conveying more moisture from the North Pacific. Further analysis indicated that an early TIO SST anomaly showed robust persistence into early summer. However, the early-summer TIO SST anomaly displayed a more significant influence on simultaneous atmospheric circulation and further affected NEC precipitation since the late 1980s. In 1989–2014, the early-summer Hadley and Ferrell cell anomalies associated with simultaneous TIO SST anomaly were much more significant and extended further north to mid-latitudes, which provided a dynamic foundation for the TIO–mid-latitude connection. Correspondingly, the TIO SST anomaly could lead to significant divergence anomalies over the Mediterranean. The advections of vorticity by the divergent component of the flow effectively acted as a Rossby wave source. Thus, an apparent Rossby wave originated from the Mediterranean and propagated east to East Asia; that further influenced the NEC precipitation through modulation to the atmospheric circulation (e.g., surface wind, moisture, vertical motion).

Keywords Tropical Indian Ocean · Northeast China's summer precipitation · Interdecadal shift · Interannual relationship

This paper is a contribution to the special issue on East Asian Climate under Global Warming: Understanding and Projection, consisting of papers from the East Asian Climate (EAC) community and the 13th EAC International Workshop in Beijing, China on 24–25 March 2016, and coordinated by Jianping Li, Huang-Hsiung Hsu, Wei-Chyung Wang, Kyung-Ja Ha, Tim Li, and Akio Kitoh.

✉ Tingting Han
hantt08@126.com

[1] Nansen-Zhu International Research Centre, Institute of Atmospheric Physics, Chinese Academy of Sciences, Beijing, China

[2] Climate Change Research Center, Chinese Academy of Sciences, Beijing, China

[3] Collaborative Innovation Center on Forecast and Evaluation of Meteorological Disasters/Key Laboratory of Meteorological Disaster, Ministry of Education, Nanjing University for Information Science and Technology, Nanjing, China

[4] University of Chinese Academy of Sciences, Beijing, China

[5] Geophysical Institute, University of Bergen and Bjerknes Centre for Climate Research, Mons, Norway

1 Introduction

The Indian Ocean is the world's third-largest ocean. The tropical Indian Ocean (TIO) is connected to the largest warm pool on earth, and it makes an important contribution to climatic changes in situ and surrounding regions via its interaction with the atmosphere (e.g., Annamalai et al.

2005; Li et al. 2006; Zhou 2011). Recent studies have indicated a greater influence of the TIO on climate variability than had previously been supposed (Schott et al. 2009).

Bounded to the north by Asia, the TIO is a major source of moisture and energy for Asian monsoon regions; thus, it exerts a substantial impact on East Asian climate (Li and Mu 2001; Xu and Fan 2012, 2014; Jiang et al. 2013; Tian and Fan 2013). Peng (2012) demonstrated that warming anomalies in the eastern TIO lead to intensification of the perturbation in the Southern Branch Trough and enhancement of moisture transportation, and then the winter precipitation increases in southern China. Wang and Chen (2012) determined that atmospheric water vapor throughout the summer in southeastern China primarily derives from the TIO.

The basin-wide warming pattern is the leading mode in the TIO, which is closely linked to the Asian climate—especially East Asian summer precipitation (Luo et al. 1985; Yan and Xiao 2000; Yuan and Zheng 2004; Chen et al. 2010; Cheng and Jia 2014; He 2015). Yang et al. (2007b) considered the significant increasing sea surface temperature (SST) trend of the Indian Ocean basin to be one reason for the weakening of the Asian summer monsoon circulation and southward shift of the summer rain band in China. Studies have revealed the influence of the SST anomaly in the TIO on the South Asian high (SAH) (e.g., Yang et al. 2007a; Li et al. 2008). Analyses of observations and atmospheric general circulation models have indicated that a warm Kelvin wave anomaly led by warming anomaly in the TIO is vital to the formation of the anomalous anticyclone over the subtropical Northwest Pacific which results in an increased Meiyu-Baiu precipitation over East Asia (Xie et al. 2009) as well as above-normal summer surface air temperature in south China and below-normal summer surface air temperature in northeast China (Hu et al. 2011). Yang et al. (2009) suggested that the warming SST anomalies in the TIO could induce a new atmospheric heating source in South Asia through a positive feedback and then generate significant circumglobal teleconnection over the mid-latitude of the Northern Hemisphere.

Recently, increasing attention has been paid to the decadal variability in the SST signals in the East Asian circulation (Wang and He 2012; He and Wang 2013a; He et al. 2013; Wang et al. 2013a, b; Fan et al. 2016; Li et al. 2017). Based on both observations and numerical simulations, Xie et al. (2010) investigated the strengthening of the TIO teleconnection with the Northwest Pacific since the mid-1970s, and they attributed the interdecadal change to the enhancement of the TIO SST variability in summer. The enhanced impact of the TIO on the SAH since the late-1970s has been confirmed by Qu and Huang (2012). The authors proposed that the change in the locations of the TIO SST anomalies and the changes in the mean SST and its variability jointly produce the distinct responses of tropospheric temperature, which accounts for the strengthening of the TIO's influence on the SAH. Yang et al. (2015) noted that the previous winter and spring SST anomaly in the TIO has exerted an intensified effect on the subsequent May precipitation in eastern Northwest China since the mid-1970s.

Located in the middle and high latitudes, Northeast China (NEC) is a major breadbasket of China. Precipitation variability in the NEC has a great impact on food production, people's lives, and social development. Recent studies have revealed that summer precipitation in NEC is influenced by atmospheric circulation anomalies over high latitudes (Han et al. 2015; Wang and He 2015) as well as over tropical oceans (Feng et al. 2006; Zhou and Wang 2014). The TIO SST anomaly is a predominant contributor to summer climate predictability over the Northwest Pacific and East Asia (Wang et al. 2013a, b; Chowdary et al. 2011; Yang et al. 2015); interdecadal changes in the ocean–atmosphere connection have been detected in many previous studies (He and Wang 2013b; Li et al. 2014a, b, 2015). Accordingly, in the present study, we aimed to investigate potential instability in the relationship between the preceding SST in the TIO and summer precipitation over NEC on the interannual time scale. We also examined the related mechanisms.

The rest of the paper is organized as follows. Section 2 describes the data sets and methods used in this study. Section 3 investigates the strengthened relationship between the early-spring SST in the TIO and precipitation in the following early summer in NEC. Conclusions appear in Sect. 4.

2 Data and methods

The monthly atmospheric reanalysis data set used in this study is the National Center for Environmental Prediction/National Center for Atmospheric Research global atmospheric reanalysis data set for 1948–2015 at a resolution of 2.5° × 2.5° (Kalnay et al. 1996). The monthly mean SST data set on a 1.0° × 1.0° latitude-longitude grid is derived from the Met Office Hadley Center for 1870–2015 (Rayner et al. 2003). An advanced monthly gridded precipitation observation data set over China (CN05.1; Wu and Gao 2013), is also used in the study. The CN05.1 data set is constructed based on information from over 2400 observation stations in China; it has a relatively high resolution of 0.5° × 0.5° for 1961–2014. That data set has been widely used in the regional climate changes and the high-resolution climate model validation (Wu et al. 2015; Zhou et al. 2016; Wang et al. 2017), which can also ensures the robustness of the precipitation anomaly related to the Indian

Ocean SST anomaly. The common time period for this study was from 1961 to 2014.

NEC is defined as the region in China north of 38°N and east of 115°E. Since the interannual variability in NEC precipitation shows consistent changes in May and June (figures not shown), this study focused on early-summer precipitation in that region.

To emphasize interannual variability, all data were filtered using the Butterworth 11-year high-pass filter before analysis. We defined the NEC precipitation (NECP) index as the normalized interannual component of area-averaged precipitation during early summer in NEC using the CN05.1 dataset. In this study, early spring refers to the mean for March and April (MA), and early summer is the average for May and June (MJ). We used Student's *t* test to detect the significance in the regression and correlation analyses.

3 Results

3.1 Strengthened relationship between early-spring SST and NECP

We observed that a barely significant relationship existed between early-summer NECP and the early-spring TIO SST, as implied by previous studies on the relationship between the spring SST anomalies in the TIO and summer precipitation in China (Zhou and Wang 2006; Jiang et al. 2009). To detect whether there exists instability in that relationship, we present in Fig. 1 the sliding correlation between the early-summer NECP index and the previous early-spring SST in the TIO. Since the sliding window is 21 years, the central year is 1971 for the period 1961–1981, for example. A positive correlation begins to appear in the northern TIO in the late 1980s. With time, that positive correlation expands southward and dominates the southern TIO after the 2000s. Figure 1 suggests that an apparently strengthened connection exists between the early-spring SST in the TIO and early-summer NECP after the late 1980s.

To facilitate our analysis, we defined the MA SST_Indian index as the normalized area-averaged SST during the early spring in the TIO (0°–30°S, 45°–120°E). The time series for the NECP index (blue solid line) and MA SST_Indian index (red dashed line) appear in Fig. 2a. It is notable that the co-variability between the two indexes is not highly consistently in-phase during the entire period. The co-variability is more apparent after the late 1980s. To illustrate this, we calculated the 21-year-sliding correlations between the two indexes. As shown in Fig. 2b, no significant correlations are observed before the late 1980s ($R=0.02$; not significant). By contrast, significant positive correlations are detected after the late 1980s ($R=0.50$; above 99% confidence interval), implying that the MA SST_Indian might have had an enhanced influence on NECP after the late 1980s. To validate the decadal change in the interannual relationship between the MA SST_Indian and NECP, we take two sub-periods based on Fig. 2: P1 (1961–1986) and P2 (1989–2014), each period consisting of 26 years. We then examined the spatial distributions of the correlation coefficients between the preceding early-spring SST anomaly in the TIO and the NECP index for the two sub-periods. During P1, the correlations do not show any areas of significance in the TIO (Fig. 3a); however, during P2, significant positive correlations are located in the TIO, especially in the southern portion (Fig. 3b). Additionally, El Niño–Southern Oscillation (ENSO) has been considered as the most striking interannual climate variability over Pacific. When the linear influence of ENSO has been removed, such decadal strengthening of the relationship between the early-spring SST anomaly in the TIO and the subsequent early-summer precipitation in NEC is replicated (figure not shown), indicating that the impact of the preceding early-spring SST anomaly in the TIO on the NECP is robust. These results confirm that the early-spring SST in the TIO is a potential driver for the interannual variability in the subsequent early-summer precipitation in NEC after the late 1980s.

3.2 Associated atmospheric circulation anomalies

To better understand the strengthened impact of the previous early-spring TIO on the NEC precipitation in the early summer after the late-1980s, we examined in this section the associated atmospheric circulation anomalies. Figure 4 displays the features of the lower-level horizontal wind anomalies during early summer associated with the MA SST_Indian and NECP indexes for the two sub-periods. During P1, warming SST anomalies in the TIO correspond to a significant anomalous anticyclone and cyclone over, respectively, the tropical western Pacific and regions south to Japan (Fig. 4a). No significant wind anomalies occur over NEC. To provide some details about the atmospheric circulation associated with the early-summer precipitation anomaly in NEC, we presented in Fig. 4c the surface wind anomaly regressed on the simultaneous NECP index. When the early-summer precipitation shows a positive anomaly, the occurrence of the anticyclonic-cyclonic-anticyclonic wind anomaly patterns can be observed longitudinally from the Sea of Okhotsk to the equatorial western Pacific. The anomalous southerly extends along East China and the anomalous southeasterly prevails over NEC. It signifies that the above-normal early-summer NECP is generally companied with anomalous southwesterly or southeasterly flows over NEC during P1. However, the early-summer

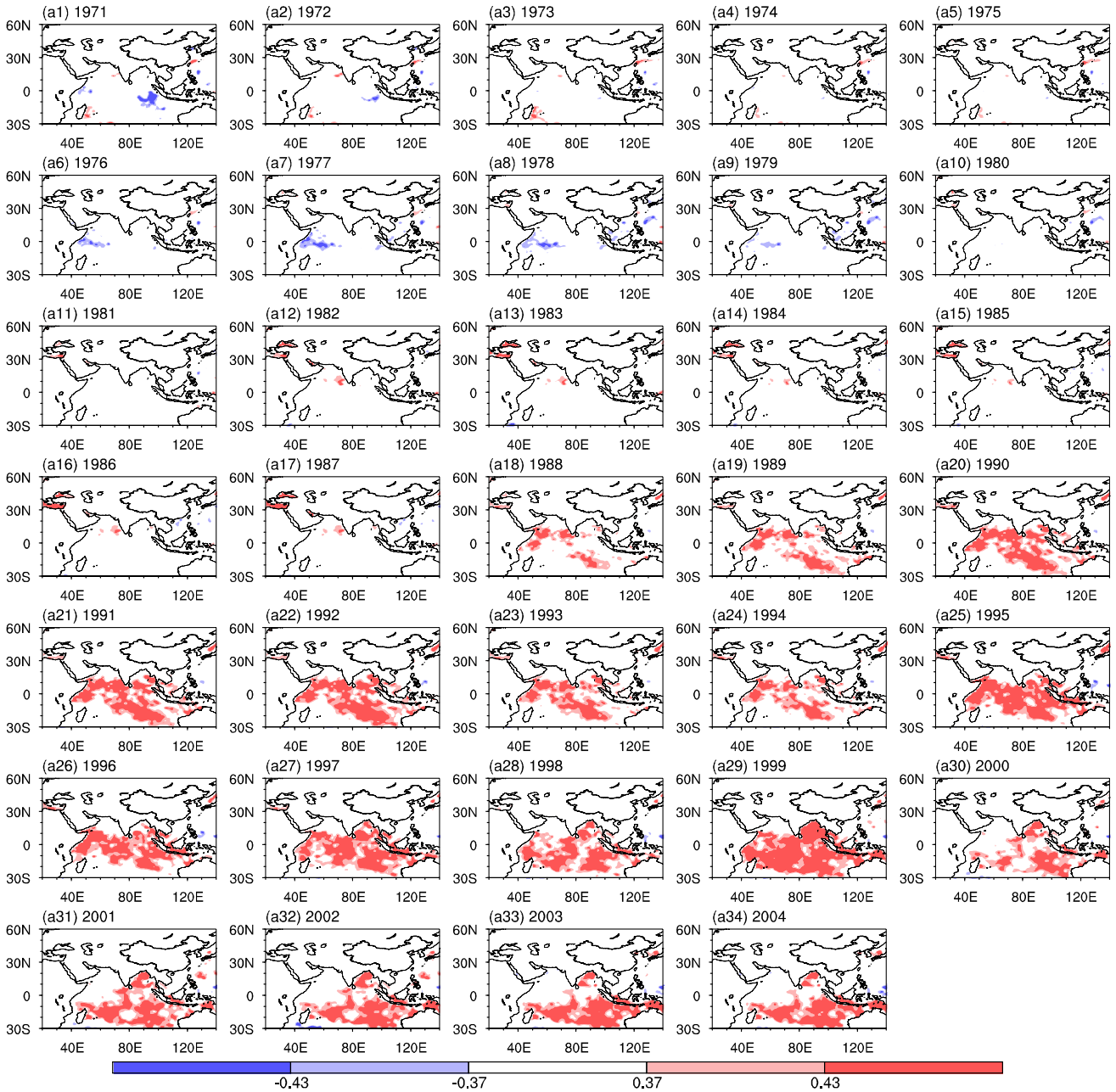

Fig. 1 Sliding correlations between the previous early-spring SST in the tropical Indian Ocean (TIO) and the early-summer precipitation in NEC (the NECP index). The sliding window is 21 years with 1-year interval. The year of each panel indicates the central year of the window. *Dark* (*light shadings*) indicate values that significantly exceeded the 95% (*90%*) confidence level, estimated using Student's *t* test

wind anomalies following the MA TIO SST anomalies are mainly confined to the western North Pacific. Consequently, the MA SST_Indian-associated horizontal wind anomalies have little influence on the early-summer precipitation in NEC.

By contrast, dramatic changes occur after the late 1980s. During P2, warming MA SST anomalies in the TIO are followed by anomalous anticyclonic wind fields over northern Europe and anomalous cyclonic wind fields over the northern Baikal region (Fig. 4b). The westerly anomalies over the Baikal region facilitate the transportation of water vapor and cold air from inland areas eastward into NEC. Additionally, an abnormal anticyclone is located over the Northwest Pacific, along with anomalous southerlies in the west flank of that anticyclone conveying warm moist air into NEC. The zonally oriented anomalous

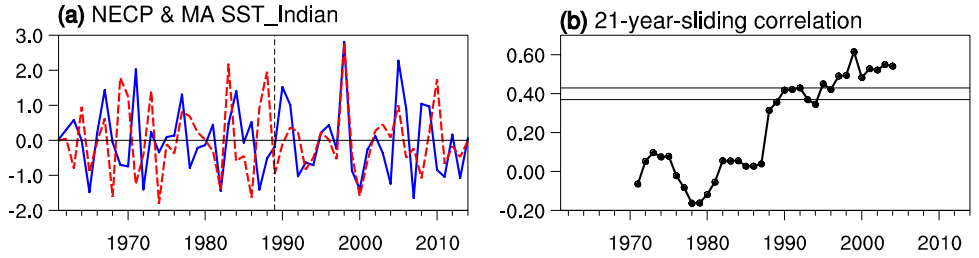

Fig. 2 **a** Time series of the normalized NECP (*blue solid line*) and MA SST_Indian (*red dashed line*) indexes for 1961–2014. **b** The 21-year-sliding correlation coefficients between the two indexes. *Horizontal black solid* lines denote 90 and 95% confidence levels estimated using Student's *t* test

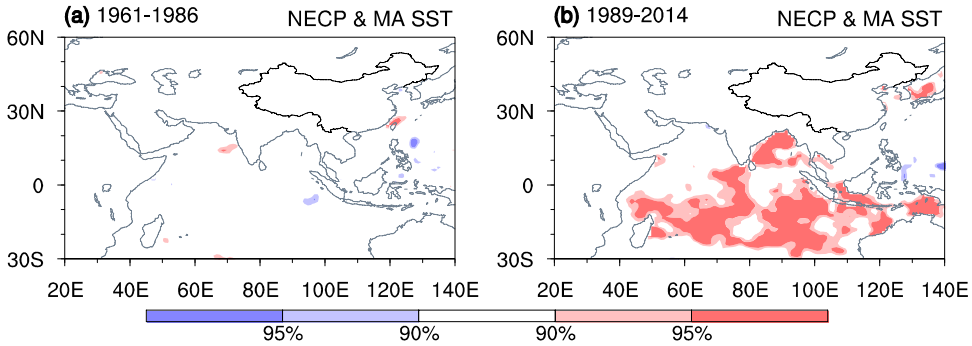

Fig. 3 Geographic distribution of the correlation coefficients between the previous early-spring SST in the TIO and the NECP index for **a** 1961–1986 and **b** 1989–2014. *Dark* (*light shadings*) indicate values that significantly exceeded the 95% (*90%*) confidence level, estimated using Student's *t* test

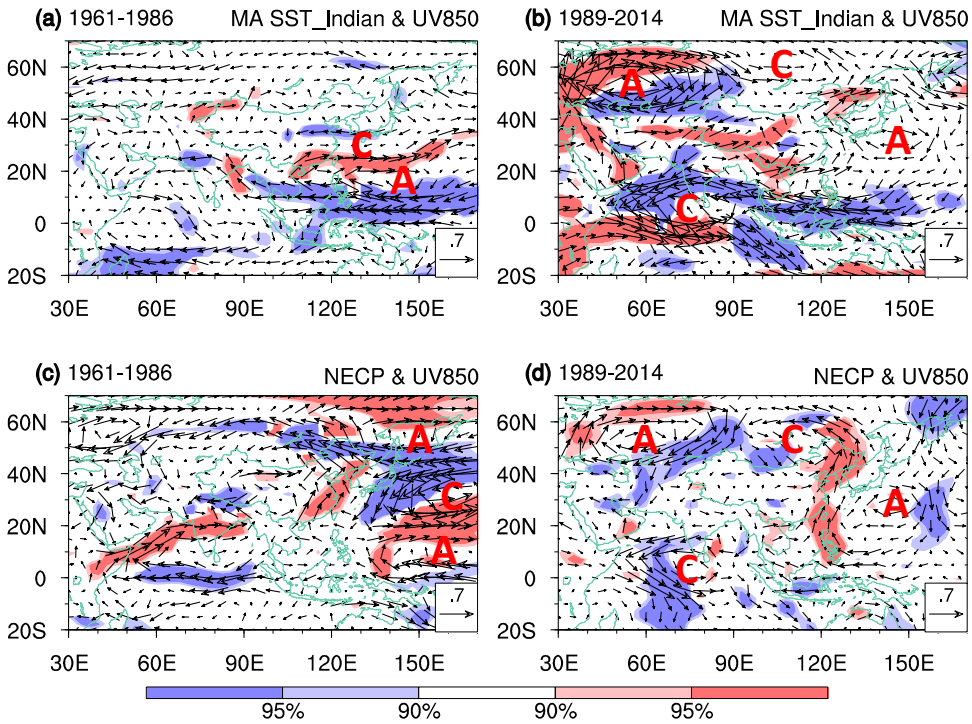

Fig. 4 Linear regression pattern of the early-summer horizontal wind at 850 hPa (UV850, unit: m s^{-1}) against the MA SST_Indian index for **a** 1961–1986 and **b** 1989–2014. **c, d** As in (**a, b**) but with the NECP index. *Dark* (*light*) *shadings* indicate values that significantly exceeded the 95% (*90%*) confidence level, estimated using Student's *t* test

anticyclone-cyclone-anticyclone pattern located in Europe, the Baikal region, and Northwest Pacific exhibits a wave-like character. It is notable that an intensified cyclone occupies the northern TIO during P2, suggesting a potential air-sea interaction over the TIO. Significant southerlies northwest to that cyclone extend northwestward to Europe, indicating that the TIO can affect the atmospheric circulation over Europe during the latter sub-period. Interestingly, the horizontal wind anomalies concurrent with the early-summer NECP agree well with those associated with the

MA TIO SST anomaly (Fig. 4d); this implies a possible effect of the MA TIO SST anomaly on the early-summer NECP.

Moisture flux is of great importance for precipitation processes (Li et al. 2011, 2012). Li and Zhou (2012) noted a significant relationship between the summer moisture circulation over East Asia–western North Pacific and SST anomalies in the Indian Ocean. Previous studies also showed that the tropical Indian Ocean and South China Sea are major water vapor sources for summer precipitation in East China (e.g., Li et al. 2014a, b; Sun and Wang 2015). Hence, the TIO SST-associated moisture conditions are explored in this section. During P1, the positive MA SST_Indian index features an anomalous moisture divergence centered over the subtropical western Pacific and an anomalous convergence of moisture centered over the Arabian Sea (Fig. 5a). The strong easterly over the tropical western Pacific transports warm wet currents across the maritime continent to the Bay of Bengal, and turns into southwesterly over south to Tibet Plateau. The anomalous southwesterly flow transports moisture from South China Sea and the Bay of Bengal to South China and the Yangtze River valley, instead of northward to NEC. Therefore, the moisture flux anomalies are tiny over NEC, and the lower-level specific humidity anomalies are insignificant over NEC (Fig. 5c). During P2, the moisture divergence over the subtropical western Pacific shifts westward and dominates the Philippines, and the convergence over the Arabian Sea becomes amplified (Fig. 5b). The anomalous easterly over the maritime continent becomes intensified, transporting water vapor from the tropical western Pacific westward to Indian. Anomalous southeasterly at the north flank of the moisture convergence turns into westerly and southwesterly that carry moisture to eastern China. In addition, there is an anomalous divergence of moisture over Japan, which is not present during P1. The peripheral southerly flow conveys water vapor deriving from the western North Pacific and invades NEC across the southern boundary, which is favorable for the increased specific humidity over NEC, especially over the western and southeastern regions (Fig. 5d). Those results indicate that the early-summer moisture anomalies that follow the MA TIO SST anomaly are more favorable for the NECP during P2 than in P1.

To illustrate the anomalous dynamic process associated with the early-summer NEC precipitation anomaly, Fig. 6 presents the vertical movement cross section along 47.5°N during the early summer associated with the MA SST_Indian index. We selected 47.5°N because that latitude is at the midpoint of the meridional orientation in NEC (38°–55°N). During P1, in response to anomalous MA SST warming in the TIO, the anomalous upward motion is statistically insignificant over NEC in early summer (Fig. 6a). However, during P2, the anomalous ascending movement becomes intensified and statistically significant;

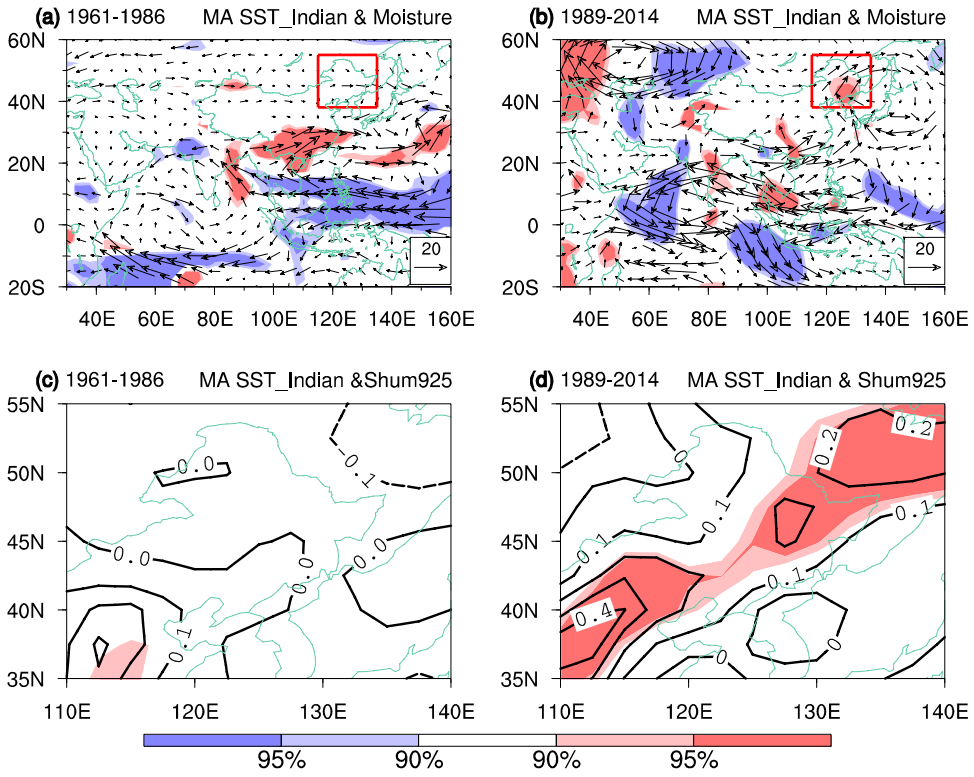

Fig. 5 Linear regression pattern of the vertically integrated moisture flux during early summer (unit: kg m^{-1} s^{-1}) against the MA SST_Indian index for **a** 1961–1986 and **b** 1989–2014. **c, d** As in **a, b** but for the specific humidity at 925 hPa (unit: k kg^{-1}). *Dark* (*light*) *shadings* indicate values that significantly exceeded the 95% (*90%*) confidence level, estimated using Student's *t* test

the strongest values are located over central NEC (Fig. 6b). Enhanced upward motion and increased moisture content are conducive to the formation of a wet climate.

3.3 Possible mechanisms

SST anomalies show good seasonal persistence because of oceanic "memory". To examine the potential persistence of the MA TIO SST anomaly, a May–June (MJ) SST_Indian index is defined as the normalized area-averaged SST during early summer in the region—as we did with the MA SST_Indian index. Figure 7a illustrates the time series of the MA and MJ SST_Indian indexes. The two indexes have consistently in-phase variabilities over the entire period (Fig. 7a), with a correlation coefficient of 0.84. The 21-year-sliding correlations between the MA and MJ SST_Indian indexes imply the strong persistence of SST anomalies in the TIO from early spring to early summer (Fig. 7b). Therefore, we speculate that the intensified connection between the early-spring TIO and early-summer NECP may be attributed to the decadal change in the simultaneous relationship between the TIO and NECP. To validate that speculation, we further investigate the relationship between the NECP and MJ SST_Indian indexes. It suggests that the NECP and MJ SST_Indian indexes do not appear to be consistently correlated (Fig. 8a): the correlation coefficient is

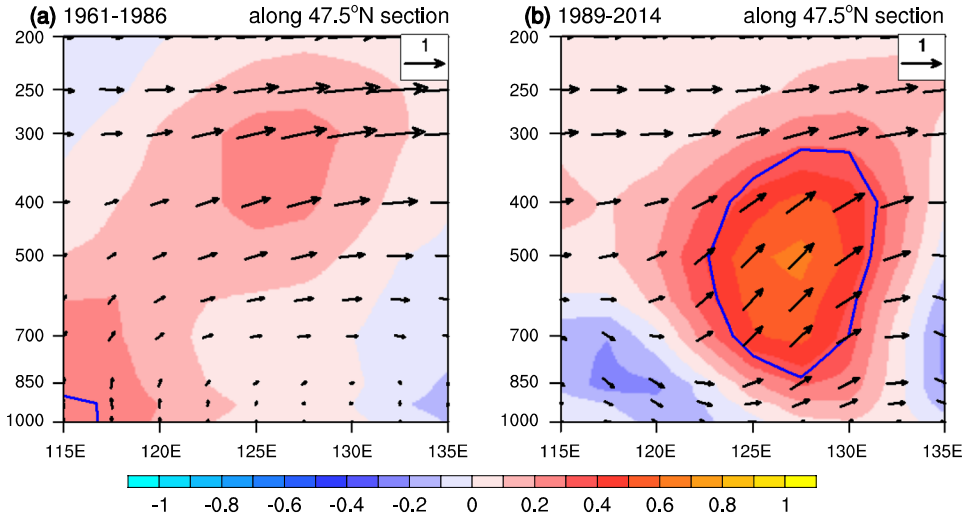

Fig. 6 Vertical-horizontal cross section along 47.5°N for vertical wind (vectors, unit: m s^{-1}) and omega (*shading*, unit: -10^{-2} Pa s^{-1}) anomalies during early summer regressed onto the MA SST_Indian index for **a** 1961–1986 and **b** 1989–2014. Omega anomalies enclosed by *blue contours* are at the 90% confidence level based on Student's *t* test

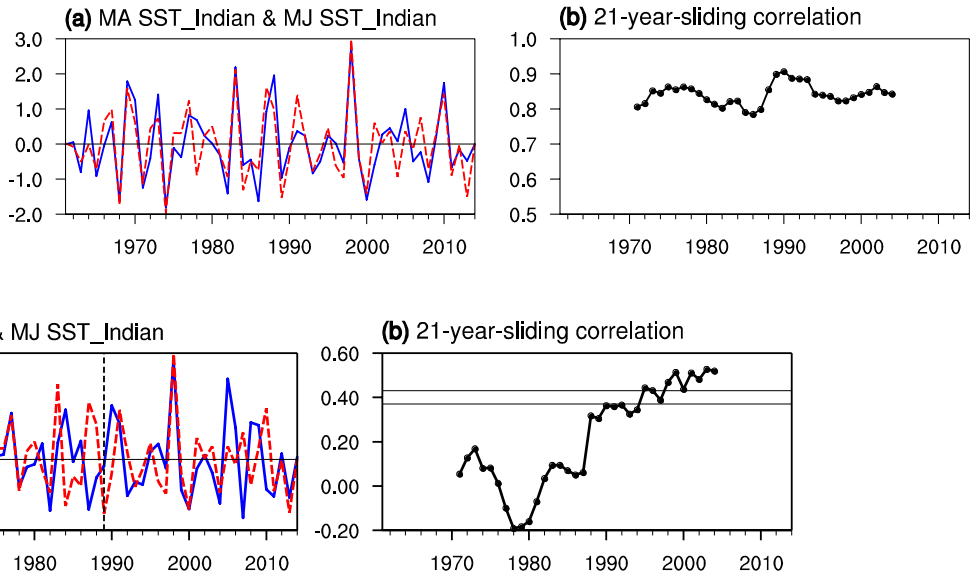

Fig. 7 **a** Time series of the MA (*blue solid line*) and MJ (*red dashed line*) SST_Indian indexes for 1961–2014. **b** The 21-year-sliding correlation coefficients between the two indexes

Fig. 8 **a** Time series of the normalized NECP (*blue solid line*) and MJ SST_Indian (*red dashed line*) indexes for 1961–2014. **b** The 21-year-sliding correlation coefficients between the two indexes. *Horizontal black solid* lines denote the 90 and 95% confidence levels estimated using Student's *t* test

about 0.22 for 1961–2014, which is barely statistically significant. After inspecting their sliding correlation, we find that the correlation coefficients are hardly significant before the late 1980s, as expected; however, they become statistically significant after that (Fig. 8b). The temporal evolution of the MJ SST_Indian index with NECP is consistent with that of the MA SST_Indian index, which primarily supports our speculation. These results indicate that the SST anomalies in the TIO can be well maintained from early spring into early summer; however, the MJ SST_Indian displays an intensified linkage to the simultaneous precipitation in NEC after the late 1980s. Therefore, the preceding early-spring SST_Indian exerts an enhanced impact on precipitation in early summer in NEC after the late 1980s.

A relevant question arises: what accounts for the decadal strengthening of the MJ SST_Indian–NECP relationship? The meridional cells are of great importance for the exchanges of mass, heat, and momentum between the tropics and mid- to- high-latitudes. Figure 9 displays the linear regression of the zonal mean mass stream function during the early summer with regard to the MJ SST_Indian index in the two sub-periods. During P1, the MJ SST_Indian index is concurrent with significant Hadley cells. The northern Ferrell cell is detected to a lesser extent. By contrast, during P2, the northern Hadley cell is quantitatively larger and spatially broader. Notably, the northern Ferrell cell becomes significant and expands poleward. However, some previous studies have revealed the preceding impacts of the spring Hadley circulation (HC) on the SST anomalies in the Indian Ocean (Zhou 2012; Zhou and Cui 2008). In order to further examine the interaction between SST anomalies in the TIO and the Hadley cell, the lead–lag correlations between the HC and MA SST_Indian are also calculated. We used the maximum positive value of the interannual zonal mean stream function occurring within the latitudinal zone of 0°–30°N to depict the intensity of the northern Hadley circulation (Zhou and Wang 2006). As can be seen in Fig. 10a, during P1, the significant correlation of the MA SST_Indian index with the HC index occurs from April, and peaks till June when MA SST_Indian leads HC by about 2–3 months. The correlations are insignificant in other months. For 1989–2014, their correlation becomes significant in January, but decreases after that, and then peaks in May when the MA SST_Indian leads HC by about 1–2 months, and then weakens (Fig. 10b). These results suggest that on the interannual time scale, the main physical process of the air-sea interaction over this region is the oceanic forcing to the atmosphere for the two subperiods. The MJ SST_Indian may have an enhanced effect on atmospheric circulation over the mid-latitudes of Eurasia through the northern cell circulations; this situation favors the connection between the tropical and mid-latitude systems.

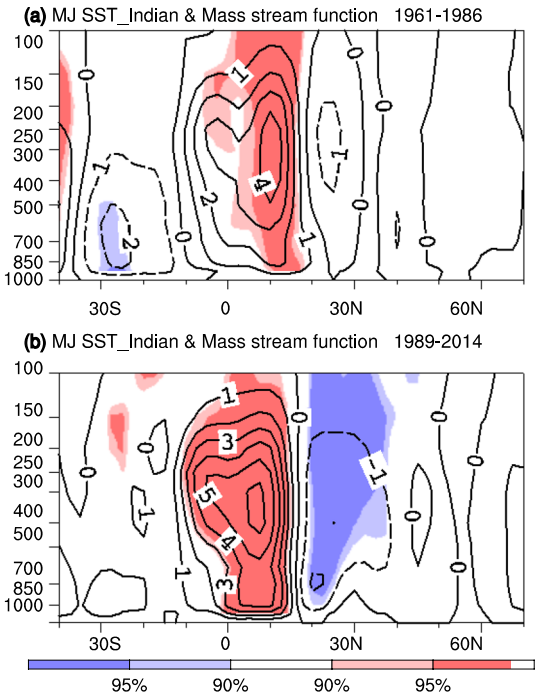

Fig. 9 Linear regression pattern of the early-summer zonal mean mass stream function (unit: 10^9 kg s^{-1}) with regard to the MJ SST_Indian index for **a** 1961–1986 and **b** 1989–2014. *Dark* (*light*) *shadings* indicate values that significantly exceeded the 95% (*90%*) confidence level, estimated using Student's *t* test

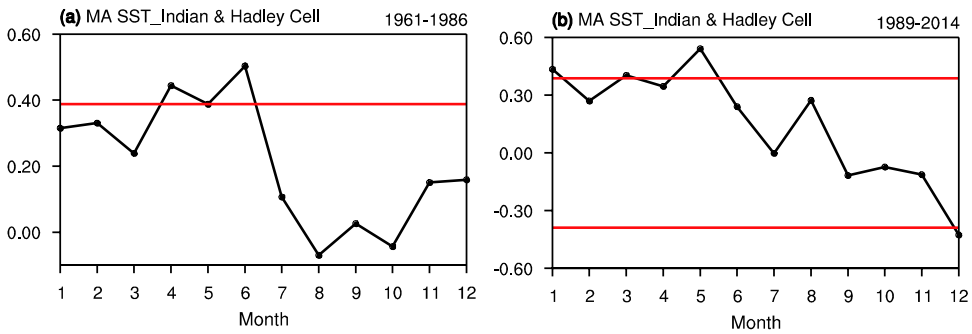

Fig. 10 Lag correlations between the MA SST_Indian index and monthly HC index for **a** 1961–1986 and **b** 1989–2014. *Horizontal dashed lines* denote 95% confidence level estimating using Student's *t* test

It should be noted that Fig. 9 provides some evidence for the dynamic mechanism for the interdecadal change in the connection between the TIO SST and mid-latitudes. However, the specific dynamic process as to how the TIO SST affects the NEC precipitation is still unavailable because the stream function is zonally averaged owing to the consideration of mass conservation. Toward providing specific details, Fig. 11 illustrates the features of the anomalous velocity potential and divergent winds in the lower and upper troposphere related to the MJ SST_Indian index. During P1, when warming SST anomalies occur, two respective divergent centers appear over the Arabian Sea and the tropical western Pacific in the lower troposphere (Fig. 11b); an anomalous convergent center is situated over the subtropical Southwest Pacific in the upper troposphere (Fig. 11a). Correspondingly, anomalous anticyclonic wind field and moisture divergence are apparent over the subtropical western Pacific (Figs. 4a, 5a). Meanwhile, anomalous upward movement is evident over the southwestern TIO (Fig. 12a). The anomalous descending and ascending motion anomalies are also observed, respectively, over the ocean east to the Philippines and the ocean south to Japan (Fig. 12a). Those results are consistent with the meridional dipolar wind anomalies over the western Pacific associated with the MA SST_Indian index (Fig. 4a). During P2, both the lower-level divergence and upper-level convergence over the western Pacific become more intense (maximum value increases) and expand poleward (Fig. 11c, d). Those results are in accordance with the occurrence of anomalous anticyclonic wind field and moisture divergence over the Northwest Pacific after the late 1980s (Figs. 4b, 5b). Notably, anomalous low-level convergence and upper-level divergence are dominant over the region stretching from the TIO to the northern Europe. Accordingly, during P2, anomalous upward movement dominates the TIO and the Mediterranean, together with downward motion prevailing over the tropical Western Pacific (Fig. 12b).

It has been suggested that heating anomalies in the TIO could lead to divergent flow over the Mediterranean in the upper troposphere (Chen and Huang 2012). Furthermore,

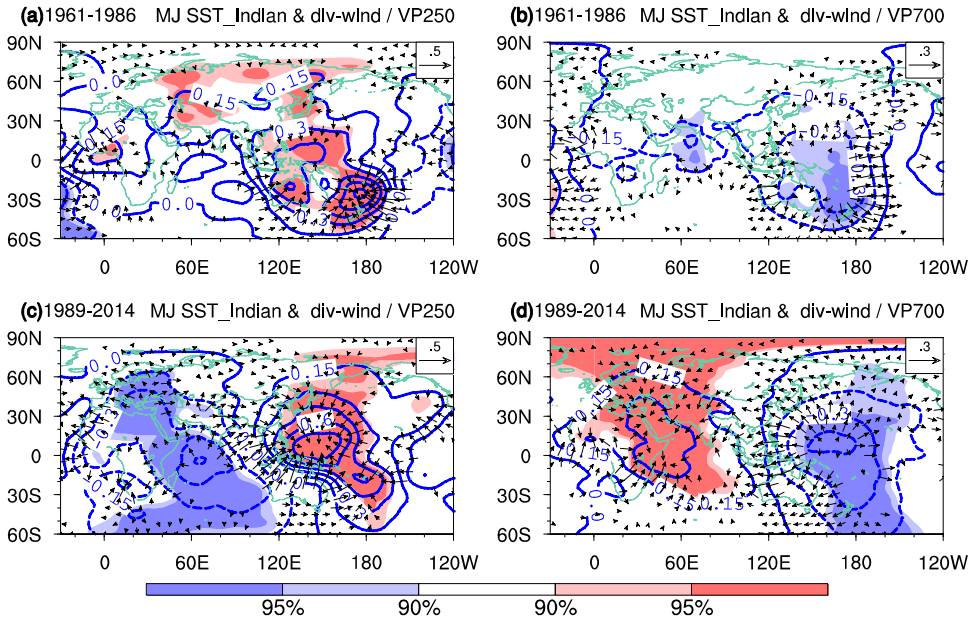

Fig. 11 Linear regression pattern of the early-summer velocity potential (unit: 10^{-6} m^2 s^{-1}) at 700 and 250 hPa with regard to the MJ SST_Indian index for **a, b** 1961–1986 and **c, d** 1989–2014. Vectors indicate divergent wind component (unit: m s^{-1}) and are significant at the 90% confidence level, as estimated using Student's *t* test. *Dark* (*light*) *shadings* indicate values that significantly exceeded the 95% (*90%*) confidence level, estimated using Student's *t* test

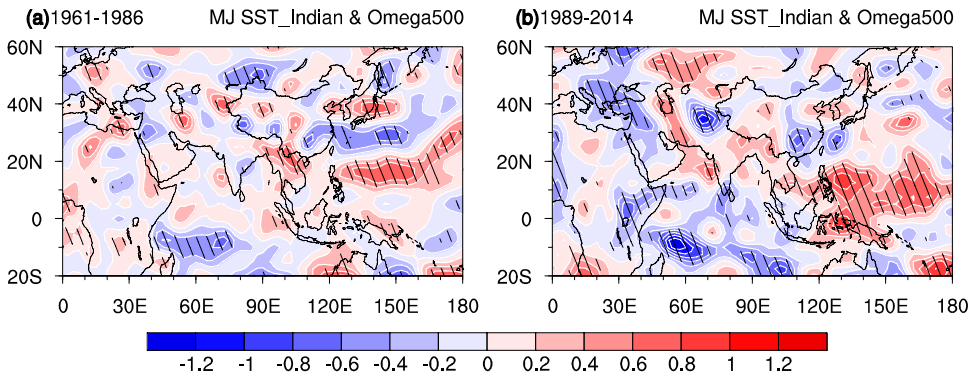

Fig. 12 Linear regression pattern of the early-summer vertical velocity at 500 hPa (unit: 10^{-2} Pa s^{-1}) against the MJ SST_Indian index for **a** 1961–1986 and **b** 1989–2014. The negative values represent upward motion, and vice versa. The *hatched areas* indicate 90% confidence level estimated using Student's *t* test

the advections of vorticity by the divergent component of the flow act as an effective Rossby wave source (Sardeshmukh and Hoskins 1988). From this perspective, it is possible that the TIO SST anomaly could induce an eastward propagating Rossby wave in P2, though it fails to do so in P1. This is evident in Fig. 13, which displays the linear regression pattern of the 300-hPa quasi-geostrophic stream function and the related wave activity flux (WAF) with regard to the MJ SST_Indian index during the two sub-periods. The WAF is computed according to Plumb's formulation (Plumb 1985), and it can describe the propagation of stationary Rossby waves. Associated with warming MJ SST_Indian anomalies during P2, an apparent eastward propagation of a Rossby wave is visible over the mid-latitudes of Eurasia; having originated in the Mediterranean Sea, it then diffused into Northeast Asia (Fig. 13b, vectors). This wave pattern could also be recognized in the associated stream function anomaly field. The alternative occurrence of negative-positive-negative-positive anomalies exhibits a wave-like pattern, extending from Eurasia eastward toward to the Sea of Okhotsk (Fig. 13b, contours). However, during P1, no evident wavelike pattern occurs over the mid-latitudes of Eurasia in the upper troposphere (Fig. 13a).

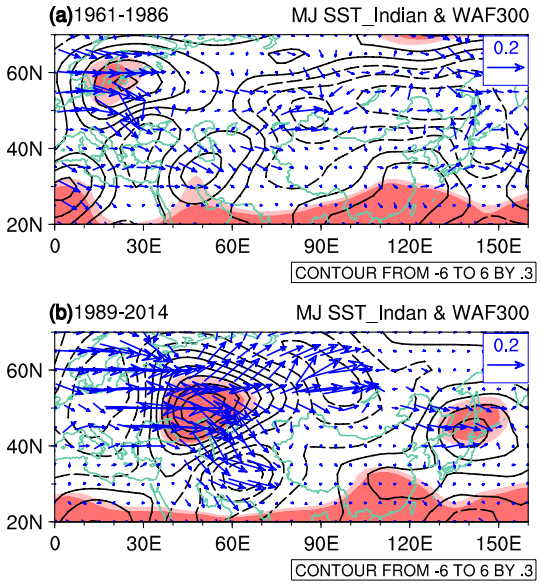

Fig. 13 Regression maps of the early-summer wave activity flux (vectors, unit: $m^2\ s^{-2}$) and quasi-geostrophic stream function (contours, unit: $10^6\ m^2\ s^{-1}$) at 300 hPa with regard to the MJ SST_Indian index for **a** 1961–1986 and **b** 1989–2014. *Dark* (*light*) *shadings* indicate values that significantly exceeded the 95% (*90%*) confidence level, estimated using Student's *t* test

4 Conclusions

This study investigates temporal variations in the connection between the early-spring TIO SST with the early-summer NECP for 1961–2014. We observed a dramatically different correlation distribution in the TIO. The TIO SST anomaly in early spring shows a significant positive correlation with NEC precipitation in early summer during 1989–2014. However, for 1961–1986, the correlation is statistically insignificant. Further analysis indicates that the early-spring positive TIO SST anomaly for 1989–2014 is generally followed by a significant anomalous anticyclone over Japan, which favors anomalous southerly wind over NEC and brings more water vapor from the North Pacific.

The SST anomalies in the TIO are well maintained from early spring to early summer throughout the entire period. After the late-1980s, the north Hadley and Ferrell cells associated with the TIO SST anomaly become more significant and extend northward to mid-latitudes; thereby, the TIO SST anomaly may have exerted an enhanced influence on atmospheric circulation over the mid-latitudes of Eurasia. Correspondingly, the associated divergence anomaly over the western Pacific becomes intensified and expands poleward, which induce the occurrence of anomalous wind fields and moisture fluxes over the Northwest Pacific after the late 1980s (Figs. 4b, 5b). Additionally, the TIO SST anomaly can also have led to a significant divergence anomaly over the Mediterranean. The advection of vorticity by the divergent component of the flow induces an effective Rossby wave source (Sardeshmukh and Hoskins 1988). Thus, a significant Rossby wave originates from the Mediterranean and propagates eastward to East Asia; that leads to anomalous atmospheric circulation over the mid-latitudes of Eurasia, which then produces the precipitation anomaly over NEC.

The precursor of East Asian (including China) summer precipitation in the tropic ocean has been explored by many previous studies (Yuan et al. 2008a, b; Feng et al. 2011; Chen et al. 2012). Yuan et al. (2008a) found that the Indian Ocean Dipole mode impacts the onset and activities of the South China Sea summer monsoon in the following year via influencing the anomalous South Asian High and subtropical high over the western Pacific. Additionally, Yuan et al. (2008b) investigated the impacts of the basin-scale Indian Ocean SST anomaly on the South China Sea summer monsoon onset. They proposed that the spring warming (cooling) SST anomalies in the Indian Ocean contribute to a later (an earlier) South China Sea summer monsoon through an intensified (a weakened) Philippines Sea anticyclone. The intensification and location of the anticyclone also result in summer precipitation anomalies in China via anomalous moisture transport and subtropical high activity, which has been reported by Feng et al. (2011). These

studies imply that the Indian Ocean SST might be a useful predictor for the East Asian summer precipitation. In our study, it is revealed that the relationship between the early-spring TIO SST and the early-summer NECP is unstable. It means that such changes should be taken into account in the climate prediction. Additionally, the result in this study is mainly based on observations and diagnostic analysis, and modelling studies are required to further explore the physical dynamics.

Acknowledgements This work was jointly supported by the National Key Research and Development Program of China (2016YFA0600703) and the National Natural Science Foundation of China (41421004).

References

Annamalai H, Liu P, Xie SP (2005) Southwest Indian Ocean SST variability: its local effect and remote influence on Asian monsoons. J Clim 18:4150–4167

Chen GS, Huang RH (2012) Excitation mechanisms of the teleconnection patterns affecting the July precipitation in Northwest China. J Clim 25:7834–7851

Chen XT, Li SL, Li GP (2010) The opposite impact of tropical Indian Ocean and Pacific Ocean warming on the East Asian summer monsoon. Trans Atmos Sci 33:624–633

Chen HP, Sun JQ, Chen XL, Zhou W (2012) CGCM projections of heavy rainfall events in China. Int J Climatol 32:441–450

Cheng HP, Jia XJ (2014) Influence of sea surface temperature anomalies of Indian Ocean in winter on precipitation over China in Spring. Plateau Meteorol 33:733–742

Chowdary JS et al (2011) Predictability of Northwest Pacific climate during summer and the role of the Tropical Indian Ocean. Clim Dyn 36:607–621

Fan K, Xie ZM, Xu ZQ (2016) Two different periods of high dust weather frequency in northern China. Atmos Oceanic Sci Lett 9:263–269

Feng X, Wang X, Wang Y (2006) Anomalies of the Northeast China floods season precipitation and SVD analysis with SSTA in world oceans. J Tropical Meteorol 22:367–373

Feng J, Chen W, Tan CY, Zhou W (2011) Different impacts of El Niño and El Niño Modoki on China rainfall in the decaying phases. Int J Climatol 31:2091–2101

Han TT, Chen HP, Wang HJ (2015) Recent changes in summer precipitation in Northeast China and the background circulation. Int J Climatol 35:4210–4219

He SP (2015) Potential connection between the Australian summer monsoon circulation and summer precipitation over central China. Atmos Oceanic Sci Lett 8:120–126

He SP, Wang HJ (2013a) Oscillating relationship between the East Asian winter monsoon and ENSO. J Clim 26:9819–9838

He SP, Wang HJ (2013b) Impact of the November/December Arctic Oscillation on the following January temperature in East Asia. J Geophys Res 118:12981–12998

He SP, Wang HJ, Liu JP (2013) Changes in the Relationship between ENSO and Asia-Pacific Mid-latitude Winter Atmospheric Circulation. J Clim 26:3377–3393

Hu KM, Huang G, Huang RH (2011) The impact of tropical Indian Ocean variability on summer surface air temperature in China. J Clim 15:5365–5377

Jiang ZH, Yang JH, Zhang Q (2009) Influence study on spring Indian Ocean SSTA to summer extreme precipitation events over the eastern part of Northwest China. J Tropical Meteorol 25:641–648

Jiang XL, Gong YF, Ma ZG, Zhang Y (2013) Relationship between leading mode of atmospheric heat sources over tropical Indian Ocean and precipitation in Eastern China during summer. J Tropical Meteorol 29:841–848

Kalnay E et al (1996) The NCEP/NCAR 40-year reanalysis project. Bull Am Meteorol Soc 77:437–471

Li CY, Mu MQ (2001) The dipole in the equatorial Indian Ocean and its impact on climate. Chin J Atmos Sci 25:433–443

Li XZ, Zhou W (2012) Quasi-4-yr coupling between El Niño-Southern Oscillation and water vapor transport over East Asia-WNP. J Clim 25:5879–5891

Li SL, Hoerling MP, Peng S (2006) Coupled ocean-atmosphere response to Indian Ocean warmth. Geophys Res Lett 33:L07713

Li SL, Lu J, Huang G, Hu KM (2008) Tropical Indian Ocean basin warming and East Asian summer monsoon: a multiple AGCM study. J Clim 21:6080–6088

Li XZ, Wen ZP, Zhou W (2011) Long-term change in summer water vapor transport over South China in recent decades. J Meteorol Soc Japan 89:271–282

Li XZ, Wen ZP, Zhou W, Wang DX (2012) Atmospheric water vapor transport associated with two decadal rainfall shifts over East China. J Meteorol Soc 90:587–602

Li F, Wang HJ, Liu JP (2014a) The strengthening relationship between Arctic Oscillation and ENSO after the mid-1990s. Int J Climatol 34:2515–2521

Li XZ, Zhou W, Chen DL, Li CY, Song J (2014b) Water vapor transport and moisture budget over Eastern China: remote forcing from the two types of El Niño. J Clim 27:8778–8792

Li F, Wang HJ, Liu JP (2015) Modulation of Aleutian Low and Antarctic Oscillation co-variability by ENSO. Clim Dyn 44:1245–1256

Li HX, Chen HP, Wang HJ (2017) Influence of North Pacific SST on heavy precipitation events in autumn over North China. Atmos Oceanic Sci Lett 10:21–28

Luo SH, Jin ZH, Chen LT (1985) Correlation analysis between sea surface temperature in the Indian Ocean and South China Sea and summer precipitation over the middle and lower reaches of Yangtze River. Scientia Atmos Sin 9:314–320

Peng JB (2012) Influence of the sea surface temperature in the eastern Indian Ocean on the wintertime rainfall in the southern part of China. Clim Environ Res 17:327–338

Plumb RA (1985) On the three-dimensional propagation of stationary waves. J Atmos Sci 42:217–229

Qu X, Huang G (2012) An enhanced influence of tropical Indian Ocean on the South Asia High after the late 1970s. J Clim 25:6930–6941

Rayner NA et al (2003) Global analyses of sea surface temperature, sea ice, and night marine air temperature since the late nineteenth century. J Geophys Res 108:4407

Sardeshmukh PD, Hoskins BJ (1988) The generation of global rotational flow by steady idealized tropical divergence. J Atmos Sci 45:1228–1251

Schott FA, Xie SP, McCreary JP (2009) Indian Ocean circulation and climate variability. Rev Geophys 47:RG1002

Sun B, Wang HJ (2015) Analysis of the major atmospheric moisture source affecting three sub-regions of East China. Int J Climatol 35:2243–2257

Tian BQ, Fan K (2013) Factors favorable to frequent extreme precipitation in the upper Yangtze River Valley. Meteorol Atmos Phys 121:189–197

Wang HJ, Chen HP (2012) Climate control for southeastern China moisture and precipitation: Indian or East Asian monsoon? J Geophys Res 117:D12109

Wang HJ, He SP (2012) Weakening relationship between East Asian Winter Monsoon and ENSO after mid-1970s. Chin Sci Bull 57:3535–3540

Wang HJ, He SP (2015) The North China/Northeastern Asia severe summer drought in 2014. J Clim 28:6667–6681

Wang HJ, He SP, Liu JP (2013a) Present and future relationship between the East Asian winter monsoon and ENSO: results of CMIP5. J Geophys Res 118:5222–5237

Wang LW, Zheng F, Zhu J (2013b) Predicting Western Pacific subtropical high using a combined tropical Indian Ocean sea surface temperature forecast. Atmos Oceanic Sci Lett 6:405–409

Wang YJ et al (2017) Changes in mean and extreme temperature and precipitation over the arid region of northwestern China: observation and projection. Adv Atmos Sci 34:287–305

Wu J, Gao XJ (2013) A gridded daily observation dataset over China region and comparison with the other datasets. Chin J Geophys 56:1102–1111

Wu J, Zhou BT, Xu Y (2015) Response of precipitation and its extremes over China to warming: CMIP5 simulation and projection. Chin J Geophys 58:3048–3060

Xie SP et al (2009) Indian Ocean capacitor effect on Indo-Western Pacific climate during the summer following El Niño. J Clim 22:730–747

Xie SP et al (2010) Decadal shift in El Niño influences on Indo-Western Pacific and East Asian climate in the 1970s. J Clim 23:3352–3368

Xu ZQ, Fan K (2012) Possible process for influences of winter and spring Indian Ocean SST anomalies interannual variability mode on summer rainfall over eastern China. Chin. J Atmos Sci 36:879–888

Xu ZQ, Fan K (2014) Simulating the mechanism of the interannual variability mode of the Indian Ocean sea surface temperature anomalies impacting on the summer rainfall over eastern China. Clim Environ Res 19:31–40

Yan HM, Xiao ZN (2000) The numerical simulation of the Indian Ocean SSTA influence on climatic variations over Asian monsoon regions. J Tropical Meteorol 16:18–27

Yang JL et al (2007a) Impact of the Indian Ocean SST basin mode on the Asian summer monsoon. Geophys Res Lett 34:L02708

Yang MZ, Ding YL, Li WJ, Mao HQ (2007b) Leading mode of Indian Ocean SST and its impacts on Asian summer monsoon. Acta Meteorol Sin 65:527–536

Yang JL et al (2009) Basin mode of Indian Ocean sea surface temperature and Northern Hemisphere circumglobal teleconnection. Geophys Res Lett 36:L19705

Yang JL et al (2015) Analysis of relationship between sea surface temperature in tropical Indian Ocean and precipitation in east of Northwest China. Plateau Meteorol 34:690–699

Yuan JS, Zheng QL (2004) Numerical Study of the effects of persistent warmer sea surface temperature for tropical Indian Ocean on atmospheric circulation in the early summer in East Asia in 1991. J Tropical Meteorol 20:249–257

Yuan Y, Yang H, Zhou W, Li CY (2008a) Influences of the Indian Ocean Dipole on the Asian summer monsoon in the following year. Int J Climatol 28:1849–1859

Yuan Y, Zhou W, Chen JCL, Li CY (2008b) Impacts of the basin-wide Indian Ocean SSTA on the South China Sea summer monsoon onset. Int J Climatol 28:1579–1587

Zhou BT (2011) Linkage between winter sea surface temperature east of Australia and summer precipitation in the Yangtze River valley and a possible physical mechanism. Chin Sci Bull 56:1821–1927

Zhou BT (2012) Multi-model projection of the interannual relationship between spring Hadley circulation and East Asian summer circulation under global warming. Chin J Geophys 55: 3517–3526

Zhou BT, Cui X (2008) Hadley circulation signal in the tropical cyclone frequency over the western North Pacific. J Geophys Res 113:D16107

Zhou BT, Wang HJ (2006) Relationship between the boreal spring Hadley circulation and the summer precipitation in the Yangtze River valley. J Geophys Res 111:D16109

Zhou MZ, Wang HJ (2014) Late winter sea ice in the Bering Sea: predictor for maize and rice production in Northeast China. J Applied Meteorol Climatol 53:1183–1192

Zhou BT et al (2016) Changes in temperature and precipitation extreme indices over China: Analysis of a high-resolution grid dataset. Int J Climatol 36:1051–1066